A CALIBRATION ALGORITHM FOR ROBUST GENERALIZED SIDELOBE CANCELLING BEAMFORMERS

Parijat Oak and Walter Kellermann

{oak,wk}@LNT.de
Multimedia Communications and Signal Processing, University of Erlangen-Nuremberg,
Cauerstr. 7, 91058 Erlangen, Germany

ABSTRACT

Deviations from ideal microphone transfer functions degrade the performance of a beamformer, especially for differential or superdirective beamformers used for small aperture arrays, e.g. in hearing aids. An adaptive microphone calibration method is desirable in order to take time-varying effects of mismatch into account. In this paper we propose a new adaptive calibration method that exploits the Robust Generalized Sidelobe Canceller (RGSC) structure. The main advantage of the proposed method is to drive the calibrating algorithm with signals that exhibit better SNR than a single microphone signal. This improves the performance of the adaptive calibration algorithm and subsequently, of the RGSC.

1. INTRODUCTION

The performance of a beamformer deteriorates in presence of deviations from the ideal microphone transfer functions. For very small aperture applications, such as hearing aids, superdirective beamformers (SBF) or differential arrays are used [1], which are highly susceptible to microphone mismatch [2]. Hence, a microphone calibration algorithm is needed. Typically, it is carried out by determining equalizing filters which are kept fixed during the beamformer operation [2]. However, time-varying factors - e.g. aging, temperature variations - necessitate adaptive calibration.
In this paper, we propose a new adaptive calibration structure which is especially well suited for the RGSC class of beamformers [3, 4].
Section 2 describes the proposed calibration algorithm. In Section 3 implementation issues are discussed. The proposed algorithm is validated in Section 4 through simulations. Section 5 gives the conclusions.

2. CALIBRATION ALGORITHM FOR RGSC

Based on the original Generalized Sidelobe Canceller [5], Hoshuyama et al. proposed a Robust GSC [3] which reduces the strongly objectionable distortion of the desired signal ('target signal cancellation'). This concept is further refined by a DFT-domain implementation, where individual frequency bins may be considered separately [4]. The proposed calibration concept is well suited for both time-domain and DFT-domain implementations although, here, it is presented for the DFT-domain implementation only. The block diagram of the proposed calibration algorithm is shown in Fig. 1 for a single frequency bin. Note that the Adaptive Interference Canceller (AIC) is not shown here as it does not influence the calibration algorithm.

The microphone signals $X_m(\omega), m = 1, 2, \ldots, M$, of an M-microphone array are equalized using the calibrating unit (CAL) and passed to the Fixed Beamformer (FBF). The FBF weights, $W_m(\omega), m = 1, 2, \ldots, M$, are designed to satisfy the constraint which prevents distortion of the look-direction. They include delay equalization implicitly. The ABM filters, $B_m(\omega), m = 1, 2, \ldots, M$, cancel the desired signal components so that the ABM outputs $Y_{b,m}(\omega), m = 1, 2, \ldots, M$, are estimates of interference-plus-noise signals [3].

The FBF output $Y_f(\omega)$ filtered with the ABM filters $B_m(\omega)$ with $m = 1, \ldots, M$ act as inputs, $U_m(\omega), m = 1, \ldots, M$, to the calibrating algorithm (ALG). It determines the calibrating filter weights which are then copied to CAL. Without loss of generality, $X_1(\omega)$ is treated as the reference signal. The signals $U_m(\omega), m = 2, \ldots, M$ are time-shifted to compensate for the inter-microphone propagation delays corresponding to the look-direction using the delays $-\tau_m, m = 2, \ldots, M$. The delays κ_b and κ_c are used for ensuring causal filters $B_m(\omega)$ and $C'_m(\omega)$, respectively.

The following analysis justifies the use of $U_m(\omega), m = 1, \ldots, M$ for the adaptive calibration. It is carried out in the DFT domain. We assume that all signals are stationary and ergodic. Furthermore, it is assumed that only the desired signal is present. For simplicity, the delays κ_b, κ_c are set to zero leading to non-causal filters.

This research was supported by Siemens Audiologische Technik GmbH, Erlangen, Germany.

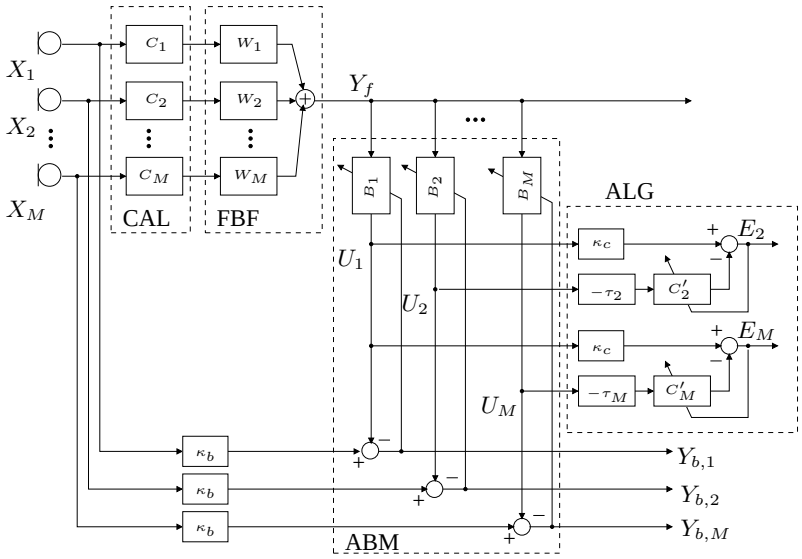

Figure 1: *Block diagram of the proposed calibration algorithm.*

2.1. Signal model

A desired source $S(\omega)$ with a known position arrives at the microphone array. Let the acoustic transfer function from the source to the m-th microphone excluding the propagation delays be denoted by $H_m(\omega)$. Then the m-th microphone signal is given by

$$X_m(\omega) = S(\omega)H_m(\omega)e^{-j\omega\tau_m}. \quad (1)$$

Using Fig. 1 and (1) the FBF output can be written as

$$Y_f(\omega) = S(\omega)\sum_{m=1}^{M} W_m(\omega)C_m(\omega)H_m(\omega)e^{-j\omega\tau_m}. \quad (2)$$

2.2. Adaptive Blocking Matrix

The m-th ABM filter transfer function $B_m(\omega)$ is determined by minimizing the power of the m-th ABM output signal $Y_{b,m}(\omega)$:

$$Y_{b,m}(\omega) = X_m(\omega) - B_m(\omega)Y_f(\omega). \quad (3)$$

Using the principle of orthogonality, the optimum filter transfer function ('Wiener Filter') is given by [6]:

$$B_m(\omega) = \frac{\Phi_{X_mY_f}(\omega)}{\Phi_{Y_fY_f}(\omega)} \quad (4)$$

where, $\Phi_{Y_fY_f}(\omega)$ is the FBF output PSD and $\Phi_{X_mY_f}(\omega)$ is the cross-power spectral density between m-th microphone signal and the FBF output. Using (1) and (2) in (4), it follows that

$$B_m(\omega) = \Phi_{SS}(\omega)\Psi(\omega)H_m(\omega)e^{-j\omega\tau_m}, \quad (5)$$

where, $\Phi_{SS}(\omega)$ denotes the PSD of the desired signal $S(\omega)$ and

$$\Psi(\omega) := \left(\sum_{m=0}^{M-1} W_m(\omega)C_m(\omega)H_m(\omega)e^{-j\omega\tau_m}\right)^* \cdot \left(\Phi_{Y_fY_f}(\omega)\right)^{-1}. \quad (6)$$

2.3. Adaptive calibrating algorithm

From the Fig. 1, we can see that

$$E_m(\omega) = U_1(\omega) - C'_m(\omega)U_m(\omega)e^{j\omega\tau_m}, \quad (7)$$

with, $m = 2, \ldots, M$. The m-th filtered FBF output signal $U_m(\omega)$ is given by

$$U_m(\omega) = B_m(\omega)Y_f(\omega). \quad (8)$$

The optimum calibrating filter is obtained by minimizing the mean square of the error signal $E_m(\omega)$. Applying the principle of orthogonality again, the optimum calibrating filter transfer function is given by

$$C'_m(\omega) = \frac{\Phi_{U_1U_m}(\omega)e^{-j\omega\tau_m}}{\Phi_{U_mU_m}(\omega)}. \quad (9)$$

With the help of (5) and (8), the optimum calibrating transfer function can be obtained as

$$C'_m(\omega) = H_1(\omega)H_m^{-1}(\omega), \quad (10)$$

provided that $\Phi_{Y_fY_f}(\omega) \neq 0$, $\Psi(\omega) \neq 0$ and $B_m(\omega) \neq 0$. The optimum filter according to (10) is identical to the one which would be obtained if the (undistorted) microphone signals $X_m(\omega)$ would be used as reference signals for identification (see [2]).

The main advantage of the proposed method is that the signals $U_m(\omega), m = 1, 2, \ldots, M$ exhibit higher SNR and less interference than a single microphone signal due to the interference suppression at the FBF stage, thereby resulting in a better performance of the adaptive algorithm [6]. The corresponding improvement in the equalization performance over known calibration methods also significantly benefits the FBF and RGSC. This is especially true when an SBF is used as the FBF.

3. IMPLEMENTATION

We implemented the proposed calibration algorithm using the DFT-domain realization of the RGSC as given in [4] using the *overlap-save* method. We use L_0-sample frames overlapped by a factor of α. This leads to the block time index $n = k\alpha/L_0$, where k is the discrete-time index. The DFT length is $2L_0$ and $\mathbf{F}$ is the $2L_0 \times 2L_0$ DFT matrix. $\mathbf{0}$ and $\mathbf{1}$ are length L row vectors. Here, only the ABM and ALG (see Fig. 1) are described. For the realization of the AIC, the reader is referred to [4].

3.1. Adaptive Blocking Matrix (ABM)

Fig. 2 shows the block diagram of the DFT-domain realization of the ABM. For simplicity, only the reference path and one ABM path are given. $2L_0$ consecutive samples of the FBF output signal $y_f(k)$ are transformed into the frequency domain as

$$\mathbf{Y}_f(n) = \text{diag}\left\{ \mathbf{F} \begin{bmatrix} y_f(n\frac{L_0}{\alpha} - 2L_0 + 1) \\ y_f(n\frac{L_0}{\alpha} - 2L_0 + 2) \\ \vdots \\ y_f(n\frac{L_0}{\alpha}) \end{bmatrix} \right\}. \quad (11)$$

Transforming the $L_0 \times 1$ ABM filter weights $\mathbf{b}_m(n)$ in the frequency domain as

$$\mathbf{B}_m(n) = \mathbf{F}\left(\mathbf{b}_m^T(n),\, \mathbf{0}\right)^T, \quad (12)$$

the $2L_0 \times 1$ error vector $\mathbf{e}_{b,m}(n)$ is computed as follows:

$$\mathbf{e}_{b,m}(n) = \mathbf{x}_m\left(n - \frac{\kappa_b \alpha}{L_0}\right) - \mathbf{P}\mathbf{F}^{-1}\mathbf{Y}_f(n)\mathbf{B}_m(n), \quad (13)$$

where, $\mathbf{P} = \text{diag}\{\mathbf{0}, \mathbf{1}\}$ and the vector $\mathbf{x}_m(n)$ is defined as

$$\mathbf{x}_m(n) = \left(\mathbf{0}, x_m\left(n\frac{L_0}{\alpha} - L_0 + 1\right), \ldots, x_m\left(n\frac{L_0}{\alpha}\right)\right)^T \quad (14)$$

With the frequency-domain block error matrix $\mathbf{E}_{b,m}(n) = \mathbf{F}\,\mathbf{e}_{b,m}(n)$, the update equation for $\mathbf{B}_m(n)$ can be written as

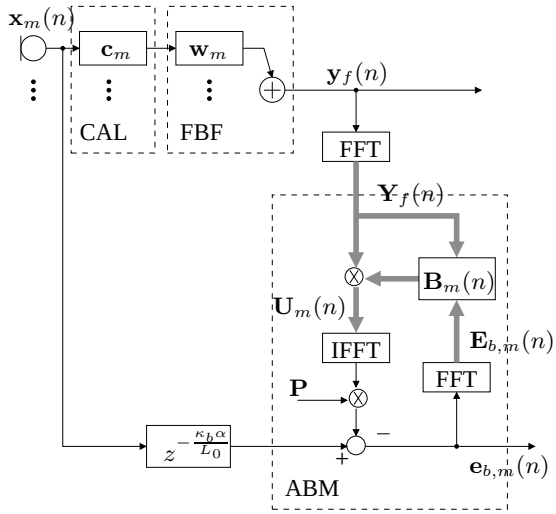

Figure 2: *Implementation of the ABM in the DFT domain.*

$$\mathbf{B}_m(n) = \mathbf{B}_m(n-1) + \mathbf{G}\boldsymbol{\mu}_b(n)\mathbf{Y}_f^H(n)\mathbf{E}_{b,m}(n). \quad (15)$$

The matrix $\mathbf{G} = \mathbf{F}\mathbf{g}\mathbf{F}^{-1}$ with $\mathbf{g} = \text{diag}\{\mathbf{1}, \mathbf{0}\}$ is a constraint matrix to avoid circular convolution effects. $\boldsymbol{\mu}_b(n)$ is a $2L_0 \times 2L_0$ diagonal matrix with normalized frequency dependent step-sizes defined as

$$\boldsymbol{\mu}_b(n) = \mu_{0,b}\,\mathbf{S}_{Y_fY_f}(n)^{-1}. \quad (16)$$

$\mathbf{S}_{Y_fY_f}(n)$ is the diagonal matrix that contains the estimated samples of the PSD $\Phi_{Y_fY_f}(\omega)$ at time n and is computed as follows:

$$\begin{aligned} \mathbf{S}_{Y_fY_f}(n) &= \lambda_b \mathbf{S}_{Y_fY_f}(n-1) + \\ &\quad (1-\lambda_b)\mathbf{Y}_f^H(n)\mathbf{Y}_f(n). \end{aligned} \quad (17)$$

One block of length L_0/α of the m-th time-domain ABM output signal $\mathbf{y}_{b,m}(n)$ is obtained by saving the last L_0/α samples of the block error signal vector $\mathbf{e}_{b,m}(n)$.

3.2. Adaptive calibration algorithm (ALG)

Fig. (3) shows the ALG adaptation. The filtered FBF output signal vector $\mathbf{U}_m(n)$ of size $2L_0 \times 1$ is available as

$$\mathbf{U}_m(n) = \mathbf{Y}_f(n)\mathbf{B}_m(n). \quad (18)$$

Stacking the calibration filter DFT bins at time n, $C'_m(n,l)$, in a $2L_0 \times 1$ vector

$$\mathbf{C}'_m(n) = (C'_m(n,0), \ldots, C'_m(n, 2L_0 - 1))^T, \quad (19)$$

the frequency-domain error vector $\mathbf{E}_m(n)$ is computed as follows:

$$\mathbf{E}_m(n) = \mathbf{U}_0 - \mathbf{U}_m(n)\mathbf{C}'_m(n), \quad (20)$$

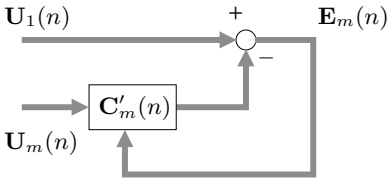

Figure 3: *Implementation of the ALG in the DFT domain.*

with, $m = 2, \ldots, M$. The update equation for $\mathbf{C}'_m(n)$ is given by

$$\mathbf{C}'_m(n) = \mathbf{C}'_m(n-1) + \mathbf{G}\boldsymbol{\mu}_c(n)\mathbf{U}^H_m(n)\mathbf{E}_m(n), \quad (21)$$

where $\boldsymbol{\mu}_c(n)$ is defined according to (16) with $\mu_{0,b}$ and $\mathbf{S}_{Y_f Y_f}(n)$ replaced by $\mu_{0,c}$ and $\mathbf{S}_{U_m U_m}(n)$, respectively:

$$\begin{aligned}\mathbf{S}_{U_m U_m}(n) &= \lambda_c \mathbf{S}_{U_m U_m}(n-1) + \\ &\quad (1-\lambda_c)\mathbf{U}^H_m(n)\mathbf{U}_m(n). \quad (22)\end{aligned}$$

3.3. Adaptation control

The proposed calibration algorithm equalizes the microphones for the target signal direction. In order to prevent it from matching the microphones for the interferer direction, the algorithm has to be adapted when the SNR is high, which denotes the presence of only the target signal. Since the ABM adaptation is also performed for the same condition, both the ABM and the calibration algorithm are adapted simultaneously. However, as the performance of the calibration algorithm depends on the ABM convergence, it should be adapted with smaller step-size than ABM: $\mu_{0,c} < \mu_{0,b}$.

4. EXPERIMENTAL EVALUATION

The algorithm was tested for a 3-microphone hearing aid with microphone spacing equal to 8 mm. The speech signals used for the simulations were recorded in a cafeteria ($T_{60} \approx 1.2s$) with the hearing aid mounted on a dummy head. The desired signal and an interferer arrived from 0° and 90°, respectively. The input SIR was approximately 0 dB. The FBF was designed as a constrained SBF [1] with susceptibility constraint equal to 15 dB. For the simulations we used $L_0 = 256$, $\mu_{0,b} = 0.01$ and $\mu_{0,c} = 0.002$. Fig. 4 plots the Interference Rejection (IR) by the RGSC with and without calibration algorithm. It can be observed that the proposed calibration method provides typically 2 dB but sometimes upto 5 dB additional interference suppression.

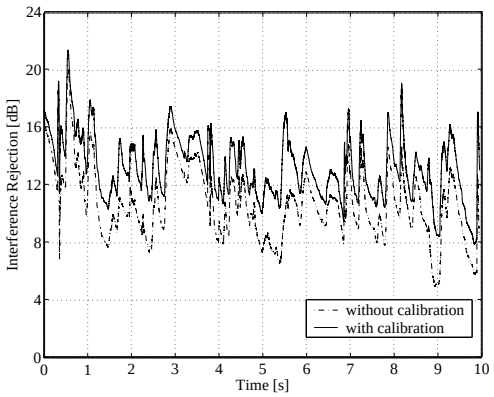

Figure 4: *Interference rejection of RGSC before and after calibration for cafeteria environment*

5. CONCLUSION

In this paper we propose a new calibration method for RGSC that uses filtered FBF output signals for the calibration algorithm. Simulations carried out for a hearing aid in real-world environments demonstrate the benefits of the proposed method to interference suppression performance of the RGSC.

6. REFERENCES

[1] J. Bitzer and K. U. Simmer, "Superdirective microphone arrays," in *Microphone Array: Signal Processing Techniques and Applications*, M. Brandstein and D. Ward, Eds., pp. 19–38. Springer, 2001.

[2] M. Buck, "Aspects of first-order differential microphone arrays in presence of sensor imperfections," *Euro. Trans. on Telecommunications*, vol. 13, no. 2, pp. 115–122, March 2002.

[3] O. Hoshuyama, A. Sugiyama, and A. Hirano, "A robust adaptive beamformer for microphone arrays with a blocking matrix using constrained adaptive filters," *IEEE Trans. on Signal Processing*, vol. 47, no. 10, pp. 2677–2684, October 1999.

[4] W. Herbordt, H. Buchner, and W. Kellermann, "An acoustic human-machine front-end for multimedia applications," *EURASIP Jour. on Applied Signal Processing*, vol. 2003, no. 1, pp. 1–11, January 2003.

[5] L. J. Griffiths and C. W. Jim, "An alternate approach to linearly constrained adaptive beamforming," *IEEE Trans. on Antennas and Propagation*, vol. 47, no. 1, pp. 27–34, January 1982.

[6] B. Widrow and S. D. Stearns, *Adaptive signal processing*, Prentice Hall, 1985.